

UCRL-10638

University of California  
Ernest O. Lawrence  
Radiation Laboratory

TWO-WEEK LOAN COPY

*This is a Library Circulating Copy  
which may be borrowed for two weeks.  
For a personal retention copy, call  
Tech. Info. Division, Ext. 5545*

PLASTIC WAVE PROPAGATION IN RODS

Berkeley, California

## **DISCLAIMER**

This document was prepared as an account of work sponsored by the United States Government. While this document is believed to contain correct information, neither the United States Government nor any agency thereof, nor the Regents of the University of California, nor any of their employees, makes any warranty, express or implied, or assumes any legal responsibility for the accuracy, completeness, or usefulness of any information, apparatus, product, or process disclosed, or represents that its use would not infringe privately owned rights. Reference herein to any specific commercial product, process, or service by its trade name, trademark, manufacturer, or otherwise, does not necessarily constitute or imply its endorsement, recommendation, or favoring by the United States Government or any agency thereof, or the Regents of the University of California. The views and opinions of authors expressed herein do not necessarily state or reflect those of the United States Government or any agency thereof or the Regents of the University of California.

For publication in Special Technical Publication and for meeting of ASTM Symposium on Dynamic Behavior of Materials, Univ. of N. M. - Sept. 27, 1963

UCRL-10638

UNIVERSITY OF CALIFORNIA  
Lawrence Radiation Laboratory  
Berkeley, California

Contract No. W-7405-eng-48

PLASTIC WAVE PROPAGATION IN RODS

S. Rajnak and F. Hauser

June 1963

## PLASTIC WAVE PROPAGATION IN RODS

S. Rajnak<sup>1</sup> and F. Hauser<sup>2</sup>

### 1. Introduction

If one examines the mechanics of an elastoplastic wave traveling along the axis of a thin rod one can readily write down two equations relating the stress  $\sigma$ , the strain  $\epsilon$ , and the particle velocity  $v$  in terms of the independent variables, the position,  $x$  and the time  $t$ . The two equations are obtained by use of the conservation of momentum and the condition of <sup>Kinematic relations</sup> continuity on a small element. However, for a complete solution of the dependent variables one additional equation relating  $\sigma$  to  $\epsilon$  is necessary. It is the assumption as to the form of this equation that distinguishes the various plastic wave propagation theories.

For the simplest case, an elastic deformation, Hooke's Law applies

$$\frac{d\sigma}{d\epsilon} = E$$

where  $E$  is Young's modulus. Therefore, for plastic wave propagation the dependent variables  $\sigma$ ,  $\epsilon$  and  $v$  can be readily computed, the only obstacle being the mathematical intricacy introduced by complex boundary conditions.

If the stress at any point in the specimen exceeds the yield strength of the material, plastic flow will take place and an assumption as to the dynamic  $\sigma - \epsilon$  behavior will have to be made. In order to permit a simple analytical rationalization of the elastoplastic wave propagation, many investigators assumed that a unique  $\sigma - \epsilon$  relation holds for a particular material. This assumption, which is the foundation of the

---

1. Research Mathematician

2. Associate Professor of Mech. Eng., University of Calif., Berkeley, Calif.

so called strain rate independent theory of plastic wave propagation leads to the conclusion that

$$C_p = \sqrt{\frac{d\sigma}{d\varepsilon} / \rho}$$

where  $C_p$  is the velocity of the plastic wave,  $\rho$  is the density, and  $\frac{d\sigma}{d\varepsilon}$  is the slope of the stress-strain curve. <sup>(1)</sup> However, Campbell, Simmons and Dorn <sup>(2)</sup> have demonstrated that the shock in strain in crystalline materials is given exclusively by the shock in elastic strain, since the shock in plastic strain is zero as a result of the inherent inertia of dislocations. On this basis it can be shown, in contrast to the assumptions made earlier and independently by von Karman <sup>(1)</sup>, G. I. Taylor <sup>(3)</sup> and Rachmatulin <sup>(4)</sup>, that the stress wave always has the velocity of the elastic wave. This theoretical deduction is confirmed by the experimental investigations of Sternglass and Stewart <sup>(5)</sup> and Alter and Curtis <sup>(6)</sup>.

Obviously a complete statement of the equation governing the material behavior would involve the second derivative of the strain with time in order to account accurately for the acceleration of the dislocations. Campbell et al <sup>(1)</sup> have estimated that, as a result of the small inertia of dislocations the accelerative period following a shock is completed in less than  $10^{-9}$  sec. at which time the plastic strain is less than 0.003. Therefore, to a good approximation the constitutive equation can be given by:

$$\frac{\partial \varepsilon}{\partial t} = \frac{1}{E} \frac{\partial \sigma}{\partial t} + g(\sigma, \varepsilon) \tag{1}$$

where  $\frac{\partial \varepsilon}{\partial t}$  is the total strain rate,  $\frac{\partial \sigma}{\partial t}$  is the stress rate and  $g(\sigma, \varepsilon)$  is the plastic strain rate. Thus, the quasi-viscous behavior of crystalline materials as originally assumed by Malvern <sup>(7, 8)</sup> has some theoretical justification.

An attempt was made by Hauser, Simmons and Dorn<sup>(9)</sup> to determine the function  $g(\sigma, \dot{\epsilon})$  experimentally by using a modification of Kolsky's<sup>(10)</sup> small wafer technique. Their results, which are recorded in Fig. 1, confirm the nominal validity of Eqn. 1. At low impact stress the logarithm of the strain rate increases linearly with the stress in harmony with the dictates of the thermally activated dislocation intersection mechanism for plastic flow.<sup>(11)</sup> At high stresses the force on the dislocations is sufficient to permit intersection without thermal activation. In the absence of other dissipative mechanisms the speed of the dislocations could then approach the shear wave velocity. When all mobile dislocations in a crystal move with the sonic velocity, a maximum strain rate limit would be reached. Actually, because the stress field is not uniform but varies periodically due to such obstacles as grain boundaries and inclusions, there will be a local slowing down of dislocations. While the details of this mechanism are not yet clear, experimentally one finds a nearly linear relation between strain rate and stress. Fig. 1 represents a series of smoothed curves through many experimental points to permit the cataloguing of the  $g(\sigma, \dot{\epsilon})$  function on punch cards for computer use.

This report covers two aspects of the problem of plastic wave propagation: the first is whether the gradients in stress and strain are small enough in thin wafers to permit sufficiently high confidence in the reliability of such data as are given in Fig. 1. The second part attempts to answer whether calculations of plastic wave propagation based on such data are in good agreement with the experimental facts. This issue is particularly important in view of the well-established discrepancies

that are commonly encountered between theory and experimental facts when the von Karman type of analysis is attempted.

2. Solution of the Equations  
Governing Plastic Wave Propagation

The system under consideration consists of the equations:

$$\rho \frac{\partial v}{\partial t} + \frac{\partial \sigma}{\partial \alpha} = 0 \tag{2}$$

$$\frac{\partial \epsilon}{\partial t} + \frac{\partial v}{\partial \alpha} = 0 \tag{3}$$

$$\frac{\partial \epsilon}{\partial t} - \frac{1}{E} \frac{\partial \sigma}{\partial t} - g(\sigma, \epsilon) = 0 \tag{4}$$

- where
- $\rho$  = density
  - $v$  = particle velocity
  - $\sigma$  = stress
  - $t$  = time
  - $\alpha$  = Lagrangian particle coordinate
  - $\epsilon$  = total strain
  - $E$  = Young's modulus

Eqn. 1 comes from the conservation of momentum, Eqn. 2 is the equation of continuity and Eqn. 3 gives the properties of the material under consideration. These equations can be solved by the method of characteristics, e. g. see Malvern<sup>(7, 8)</sup>. The resulting equations were approximated by a finite difference technique, and the problem solved numerically on a computer. (12)

### 3. Boundary Conditions

The boundary conditions are determined by the geometry of the system and the nature of the input stress. Fig. 2 shows the geometry and boundary conditions for a thin wafer test. The strain gages are at  $x = -x_1$ ,  $x = x_3$ . Thus, the strain is known as a function of time at these points. Since the wave is elastic in the input and output bars, the stress and particle velocity along  $x = -x_1$ , and  $x = x_3$  are related to the strain by the equations  $\sigma = E\epsilon$  and  $v = \sigma/\rho c = E\epsilon/\rho c = c\epsilon$ . Prior to the impact,  $\sigma = \epsilon = v = 0$ . In Fig. 2 the time  $t = 0$  is the instant that the front of the stress wave arrives at the  $-x_1$  strain gages. In any physical system the front of the stress pulse rises continuously from  $\sigma = 0$  and the initial portion of the wave below the yield stress of the specimen will travel through the input bar and specimen with a velocity  $c$  without attenuation. The characteristic  $\xi_0$  represents the path of the wave front, along which  $\sigma = \epsilon = v = 0$ .

Across the boundary between the input bar and the specimen,  $x = 0$ , there are discontinuities in  $\sigma$  and  $\epsilon$ . The discontinuity in  $\sigma$  arises from the change in the cross-sectional area in going from the input bar to the specimen. The discontinuity in  $\epsilon$  arises from two sources: (1) the change in stress across  $x = 0$  gives a corresponding change in the elastic strain, (2) the plastic strain in the specimen will be non-zero at any time after the yield stress has been exceeded, while in the input bar the plastic strain is identically zero.

Consider a point on  $x = 0$ . Let the superscripts I and II denote region I and II, respectively. Since the specimen and the input bar are in contact, the particle velocities across the boundary are equal.

Therefore,

$$v^I = v^{II} \quad \text{along} \quad \mathcal{L} = 0$$

The relation between the stresses is obtained by equating the force on the face of the input bar to the force on the face of the specimen:

$$\sigma^{II} = \frac{A^I}{A^{II}} \sigma^I = K \sigma^I$$

where  $A^I$  and  $A^{II}$  are the cross-sectional areas of the input bar and specimen, respectively. The same analysis applies at  $\mathcal{L} = \mathcal{L}_2$ .

Fig. 3 shows the geometry and boundary conditions for the long bar test. The boundary conditions at  $\mathcal{L} = -\mathcal{L}_1$  and  $\mathcal{L} = 0$  are the same as in the case for the thin wafer test. At  $\mathcal{L} = \mathcal{L}_0$  the boundary condition is  $\sigma = 0$  for all  $t$  since the free end cannot support any stress. The method of characteristics permitted the rewriting of equations 2, 3 and 4 as essentially ordinary differential equations along the wave paths. These equations in turn were approximated by finite difference equations. The final solutions were obtained by a point by point integration of the equations in the  $\mathcal{L}, t$  plane using the appropriate boundary conditions and the experimental  $g(\sigma, \epsilon)$  function in tabular form. The computations were carried out on an electronic computer at the Lawrence Radiation Laboratory. (11)

Experimental Details:

1. Thin wafer--the material used for the specimen was 99.997% Al extruded bar stock, which was prestrained in compression to a yield strength of 11,000 psi. The input and output bars were hard Al tubes, .750" O.D. and .580" I.D.; a 0.4" gage length for the specimen was chosen since this length has given very consistent results in the determination of the g-function.

2. Long bar test--the material was the same as that used in the thin wafer test. The specimen was machined as a thin walled tube (.750 in

O.D. and .580 in I.D.) in order to reduce constraints on the longitudinal flow due to radial forces. The input end of the specimen and the output end of the input bar were coned to the experimentally determined friction angle of  $15^\circ$  to reduce the constraints on radial flow at the end of the specimen.

Plastic strains in the specimen were determined by measuring the wall thickness,  $w$  before and after impact, and using the relation

$$\epsilon = \left(1 + \frac{\Delta w}{w}\right)^2 - 1$$

This relation is obtained by assuming constancy of volume and cylindrical symmetry of the specimen.

Three longitudinal traces of the wall thickness were made,  $120^\circ$  apart. The measurements were carried out using a Statham gage. The gage was mounted via a pin to the crosshead of an Instron tensile testing machine. The signal from the gage went to the X coordinate on an XY plotter while the head travel gave the Y coordinate. A typical graph is shown in Fig. 4. Since it was desired to obtain the strain as a function of the Lagrangian coordinate  $\mathcal{L}$ , a method of locating a given  $\mathcal{L}$  after impact was necessary. This was accomplished by machining very fine circumferential marks on the surface of the specimen at intervals of approximately 0.1 in. These marks then appeared as ridges in the thickness measurements before and after impact. Thus, the  $\mathcal{L}$  coordinate of the marks was known and the coordinates of the points between the marks were found by linear interpolation.

#### 4. Results and Discussion

Thin wafer test:

The constants in the problem were taken as

$$E = 10.0 \times 10^6 \text{ psi}$$

$$\rho = 2.50 \times 10^{-4} \text{ lbs/in}^3$$

$$c = 2.0 \times 10^5 \text{ in/sec.}$$

Since the input and output bars and the specimen were aluminum,  $E$ ,  $\rho$  and  $c$  are the same in all three. The cross-sectional areas of the bars and the specimen were the same, giving  $K = 1$  at both the input and output faces. The results are summarized in Figs. 5 through 9.

Fig. 5 shows the stress at the strain gage on the input bar ( $-L_1$ ). The oscillations on the experimental wave are transverse vibrations in the input bar. These were ignored since they contribute very little to the longitudinal stress on the specimen.

Fig. 6 shows the stress at the strain gage in the output bar. Figs. 5 and 6 show excellent agreement with the experimental data except for the initial portion of the transmitted curve. The elastic rise of the transmitted stress is slower than that of input stress. This was true for most of the thin wafer tests run and is probably due to a slight mismatch between the faces of the specimen and the input and output bar. In the computation, the specimen was assumed to be in perfect contact with the input and output bars giving a perfect transmission of the input stress below 11,000 psi. The initial portion of the theoretical transmitted curve is somewhat lower than that of the experimental curve and the drop due to the reflected stresses in the theoretical input curve is faster than that of the experimental curve.

This indicates that the extrapolation of the g-function to low values of strain seems to give a strain rate which is too large for small strains.

Figs. 7 through 9 show that the theoretical stress, strain and strain rate do not achieve a linear gradient across the wafer before  $t = 20, 40$  and  $50 \mu$  seconds, respectively. The small peaks on the initial portion of the stress at the front face are due to the finite grid size used and the fact that the g-function is changing very rapidly in this region. The strain rate distribution initially shows very large fluctuations. This is due to the rapidly changing character of the g-function at low strains.

As  $t \rightarrow \infty$  the theoretical values of the variables become asymptotic to the experimental curves. Thus, the thin wafer technique will give good results in a determination of the g-function for a given material only in the region of large strains, which is equivalent to a long time. If the strain-rate variation of the material changes rather slowly as a function of strain then the accuracy of the method will be increased at lower strains.

Although the assumption of linearity in stress, strain and strain rate gradients does not hold for small strains, the excellent agreement between the experimental and theoretical stress curves at the strain gages  $\mathcal{L} = -\mathcal{L}_1$ , and  $\mathcal{L} = \mathcal{L}_3$  shows that the g-function determined by the thin wafer technique may be used to predict the gross behavior of a specimen. It should be noted that the only experimental data used in determining the g-function were the stresses at  $-\mathcal{L}_1$  and  $\mathcal{L}_3$ . Thus, even though non-linear gradients do exist across the specimen, the experimental determination, which assumed only linear gradients and really determines an 'average' g-function, gives a g-function which yields internally consistent results.

This is not as redundant as it first appears to be. If all the thin wafer tests had been with a gage section of 0.4" the above statements would be trivial. But since the determination of the g-function in different ranges was made using different gage lengths (0.1" to 1.6") the agreement between the experimental and theoretical input and output stresses for a 0.4" wafer is more than just a statement about the internal consistency of the experiment.

#### Long bar test;

The results for the long bar test are summarized in Figs. 10 through 13.  $t = 0$  is the time when the front of the stress wave reaches the front of the bar.  $t = 8 \mu$  sec. is the time for the wave to travel  $1/2$  the length of the specimen. At  $t = 16 \mu$  sec. the wave has just reached the end of the bar. Fig. 10 shows that the stress below the yield stress of 11,000 psi is propagated elastically while the stress above 11,000 psi has been dissipated by plastic straining of the material. As  $t$  increases the 11,000 psi stress is reflected from the free end as a tension pulse and the stress at the free end drops to zero. At  $t = 32 \mu$  sec. this reflection reaches the input end of the specimen. As  $t$  continues to increase the strain rate changes in such a way as to tend to equalize the stress distributions along the bar.

Fig. 13 shows excellent agreement of the final experimental and theoretical strain distributions. The strain is essentially zero for  $x > 1.8$  in. It should be noted that the specimen has not been completely unloaded from the input bar at  $t = 160 \mu$  sec., which is the last of the theoretical computations. However, since the g-function is very small at this time, the contribution to the strain for succeeding times will be negligible. A tension pulse reflected from the input face of the

specimen due to the discontinuity in cross-section area, traveled back along the input bar and reflected from the face of the ram as a tension pulse. The final unloading of the specimen took place when this pulse reached the input face of the specimen again.

The results tend to support the assumption that, although the thin wafer determination of the  $g$ -function gives only an average  $g(\sigma, \epsilon)$  function, the averaging process in fact gives the correct result for  $\epsilon > 2\%$ . (As was previously noted, the  $g$ -function for very low strains,  $\epsilon < 2\%$ , seems to be too large). In this region, some other experimental method of determining the  $g$ -function is needed. The final verification of this assumption awaits an experimental method of determining the stress, strain and strain rate over a gage section much less than 0.1 inch.

## 5. Conclusions

1. Although rather high stress, and strain-rate gradients exist initially in impacted thin wafers, the data obtained from such experiments represent the average dynamic plastic behavior of materials.

2. Predictions of plastic strains based on the quasi-viscous behavior of dynamically impacted materials agree very well with experimental observations if the stress, strain, strain-rate behavior of the material is known.

ACKNOWLEDGMENTS

The authors wish to express their appreciation to the Lawrence Radiation Laboratory for their interest in and support of this investigation. They are particularly indebted to Mr. T. Larsen for his aid in conducting the experiments and to Professor J. E. Dorn for his invaluable encouragement and counsel.

Bibliography

1. von Karman, T., Duwez, P., Sixth International Congress, Appl. Mechanics, Paris, J. Appl. Phys., 21, (Oct., 1950), p. 987.
2. Campbell, J.D., Simmons, J.A., Dorn, J.E., "On the Dynamic Behavior of a Frank-Read Source", J. Appl. Mech., 28, (Sept., 1961), p. 447.
3. Taylor, G.I., "Plastic Wave in a Wire Extended by an Impact Load," Scientific Papers, 1, Cambridge Univ. Press, (1957), p. 467.
4. Rakhmatulin, K.A., "Propagation of a Wave of Unloading," ONR Translation, #2, Brown Univ., (Nov. 1945).
5. Sternglass, E.J., and Stuart, D.A., "An Experimental Study of the Propagation of Transient Longitudinal Deformations in Elastoplastic Media," J. of Appl. Mech., 20, (1953), p. 427.
6. Alter, B.E.K. and Curtis, C.W., "Effect of Strain Rate on the Propagation of a Plastic Strain Pulse along a Lead Bar," J. Appl. Phys., 27, #9, (July, 1956), p. 1079.
7. Malvern, L.E., "Plastic Wave Propagation in a Bar of Material Exhibiting a Strain Rate Effect," Quarterly of Appl. Math., 8, #4, (Jan., 1951), p. 405.
8. Malvern, L.E., "The Propagation of Longitudinal Waves of Plastic Deformation in a Bar of Material Exhibiting a Strain-Rate Effect," J. of Appl. Mech., 18, (June, 1951), p. 203.
9. Hauser, F.E., Simmons, J.A., and Dorn, J.E., "Strain Rate Effects in Plastic Wave Propagation", Response of Metals to High Velocity Deformation Conference, Interscience Publishers, New York, (1961), p. 93.
10. Kolsky, H., Proc. Phys. Soc., 62, (1949), London, p. 677.
11. Hauser, F., Rajnak, S., Dorn, J., to be published
12. Rajnak, S., Hauser, F.E., Dorn, J.E., "Theoretical Prediction of Strain Distribution Under Impact Loading," Univ. of Calif., MRL Publication, Series 174, Issue 1, (June 1961).

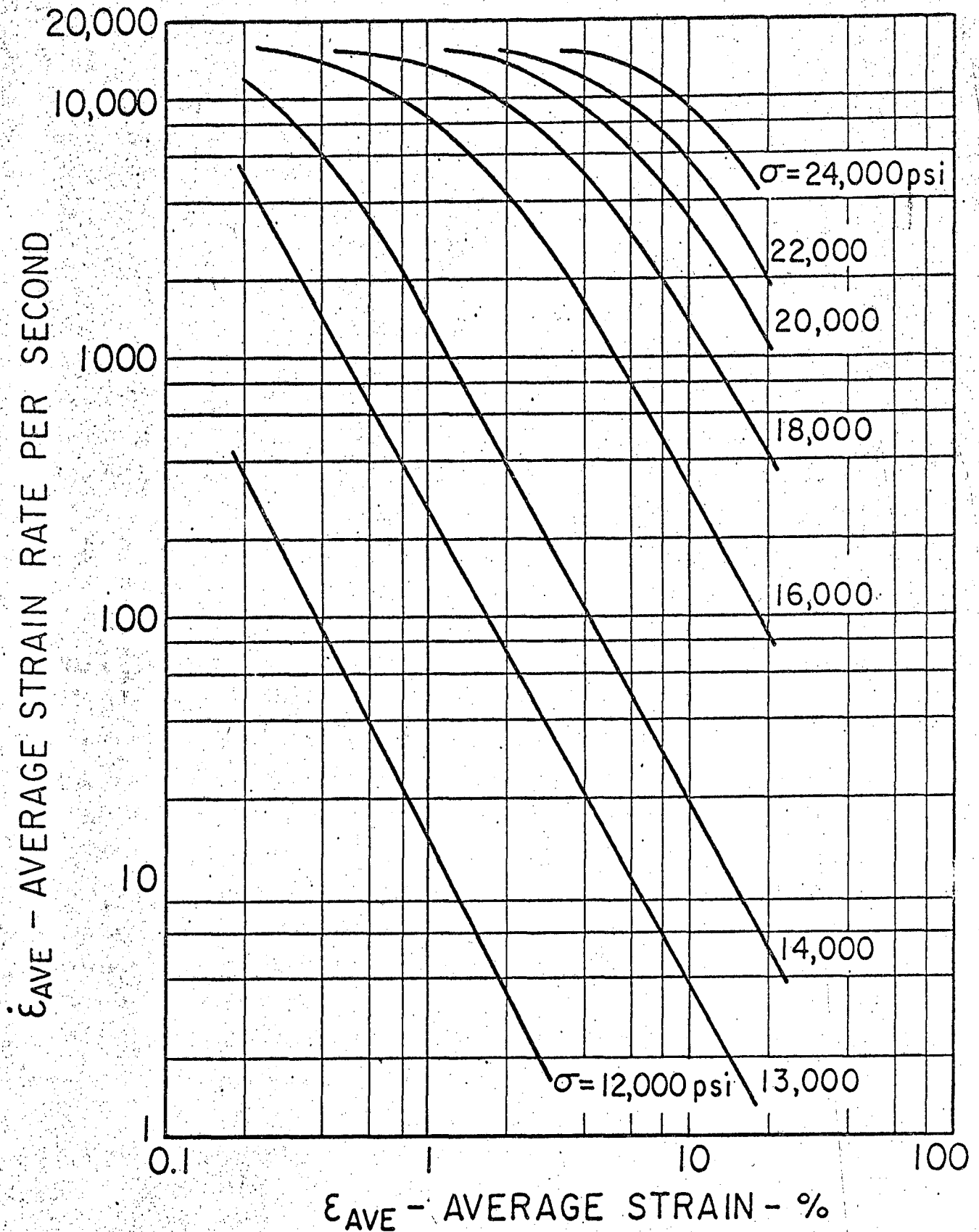
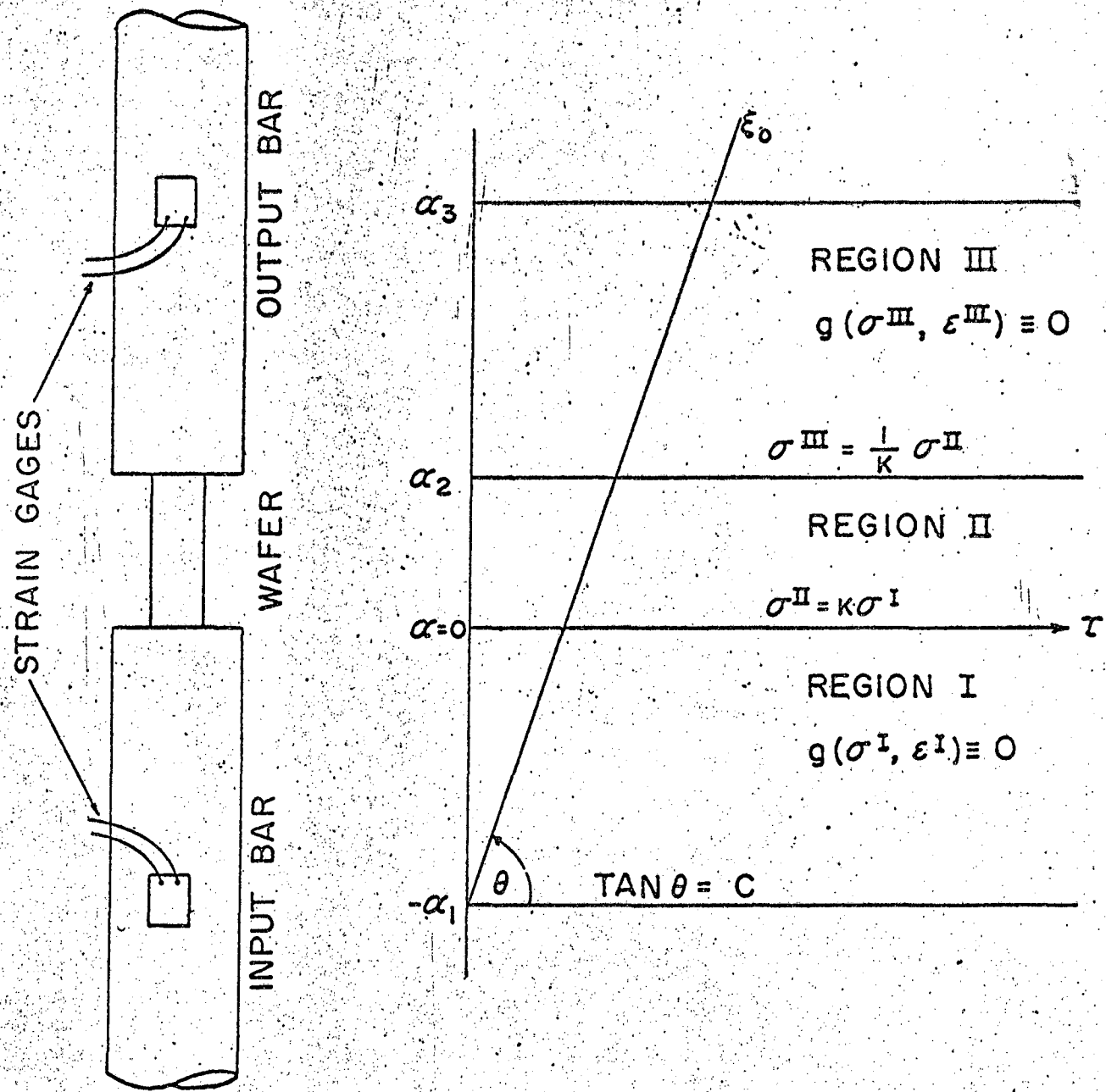
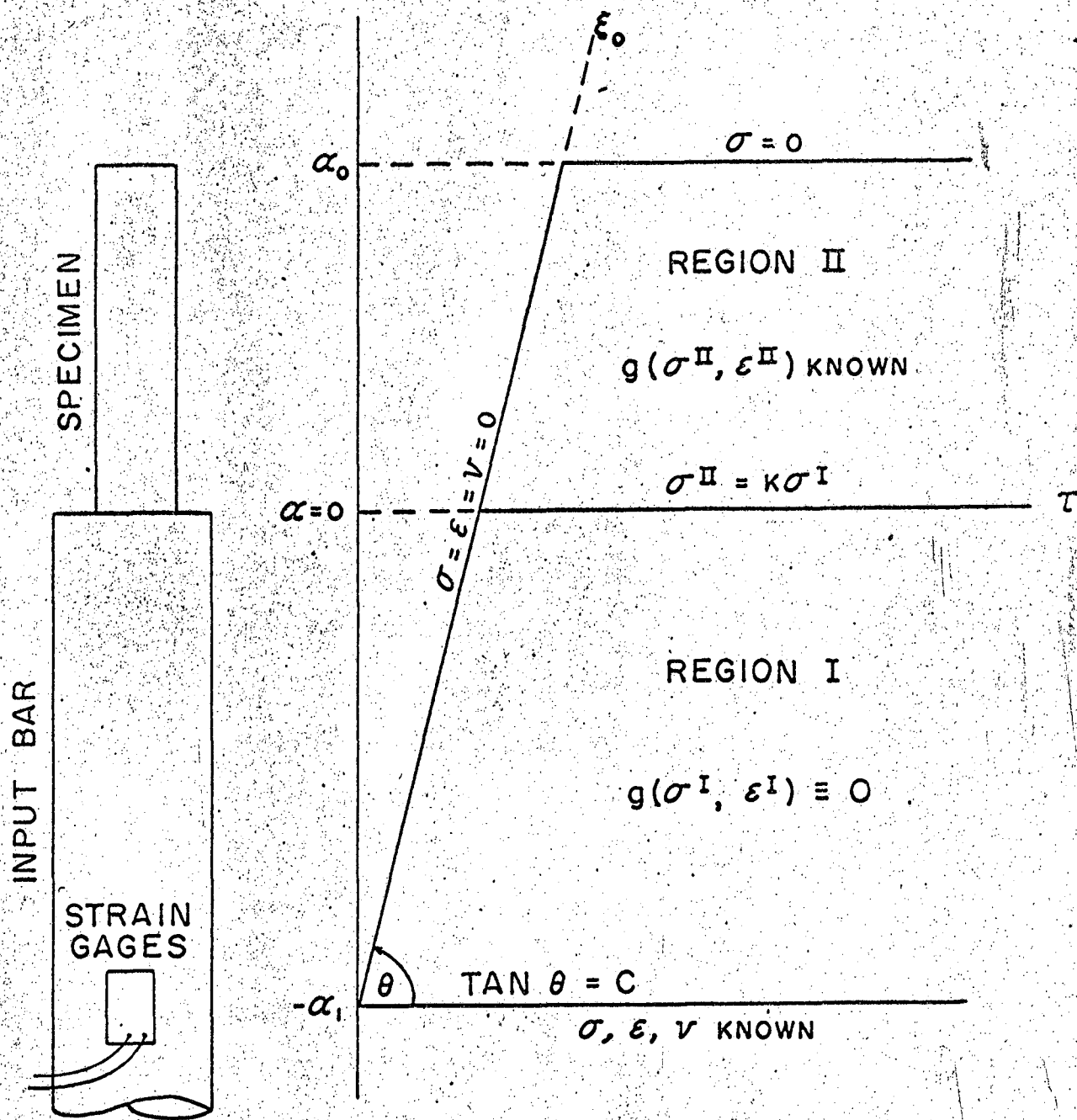


FIG.1 RELATION BETWEEN STRESS, STRAIN AND STRAIN-RATE FOR PURE Al AT  $T=295^{\circ}K$



BOUNDARY CONDITIONS FOR THIN WAFER TEST.

FIG. 2



BOUNDARY CONDITIONS FOR LONG BAR TEST.

FIG. 3

NUMBERS SHOW CORRESPONDING POINTS

.0012

.1

AFTER IMPACT

BEFORE IMPACT

-18-

FIG. 4 THICKNESS MEASUREMENT.

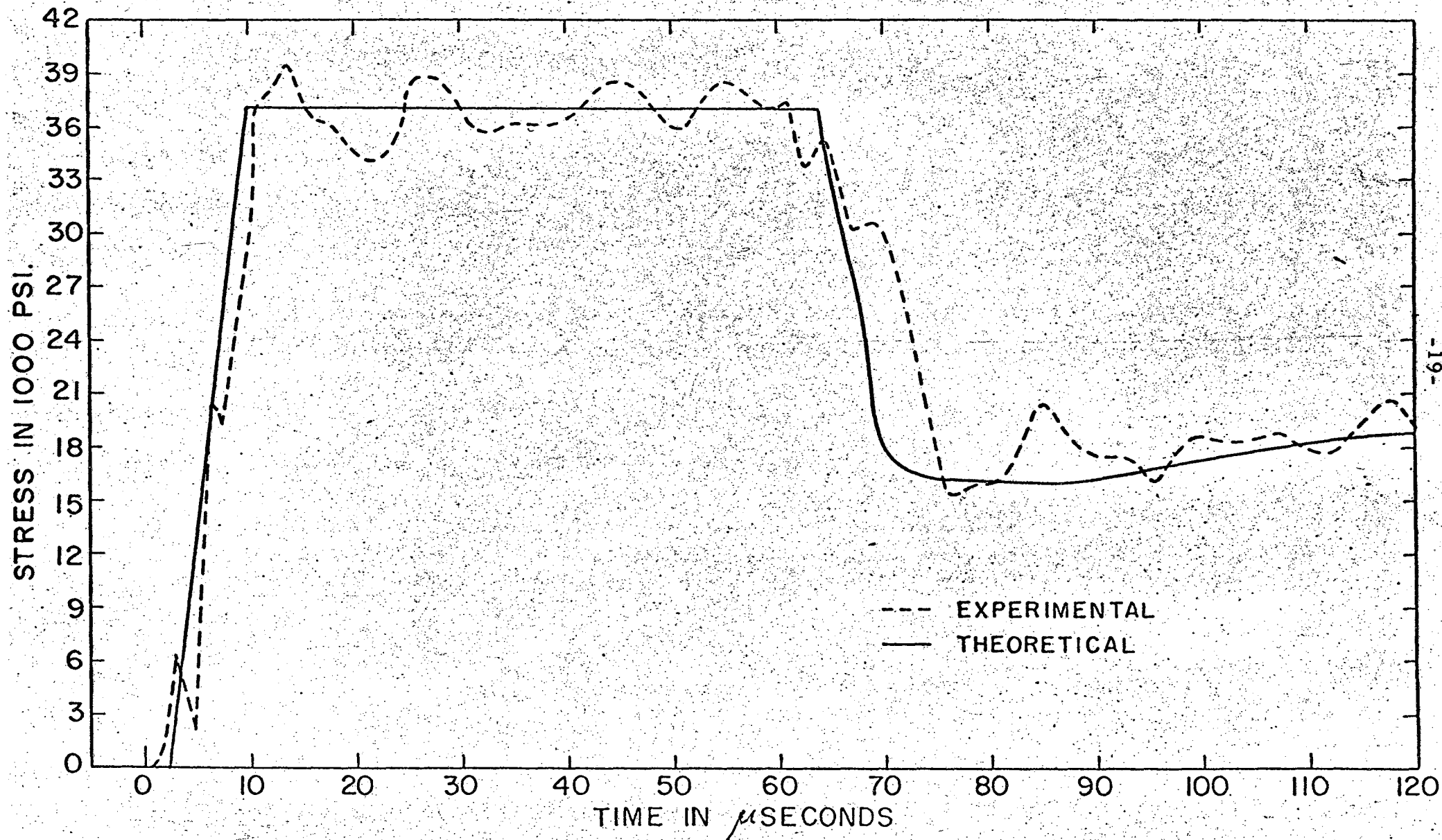


FIG. 5 STRESS AT  $-\alpha_1$  IN THIN WAFER TEST.

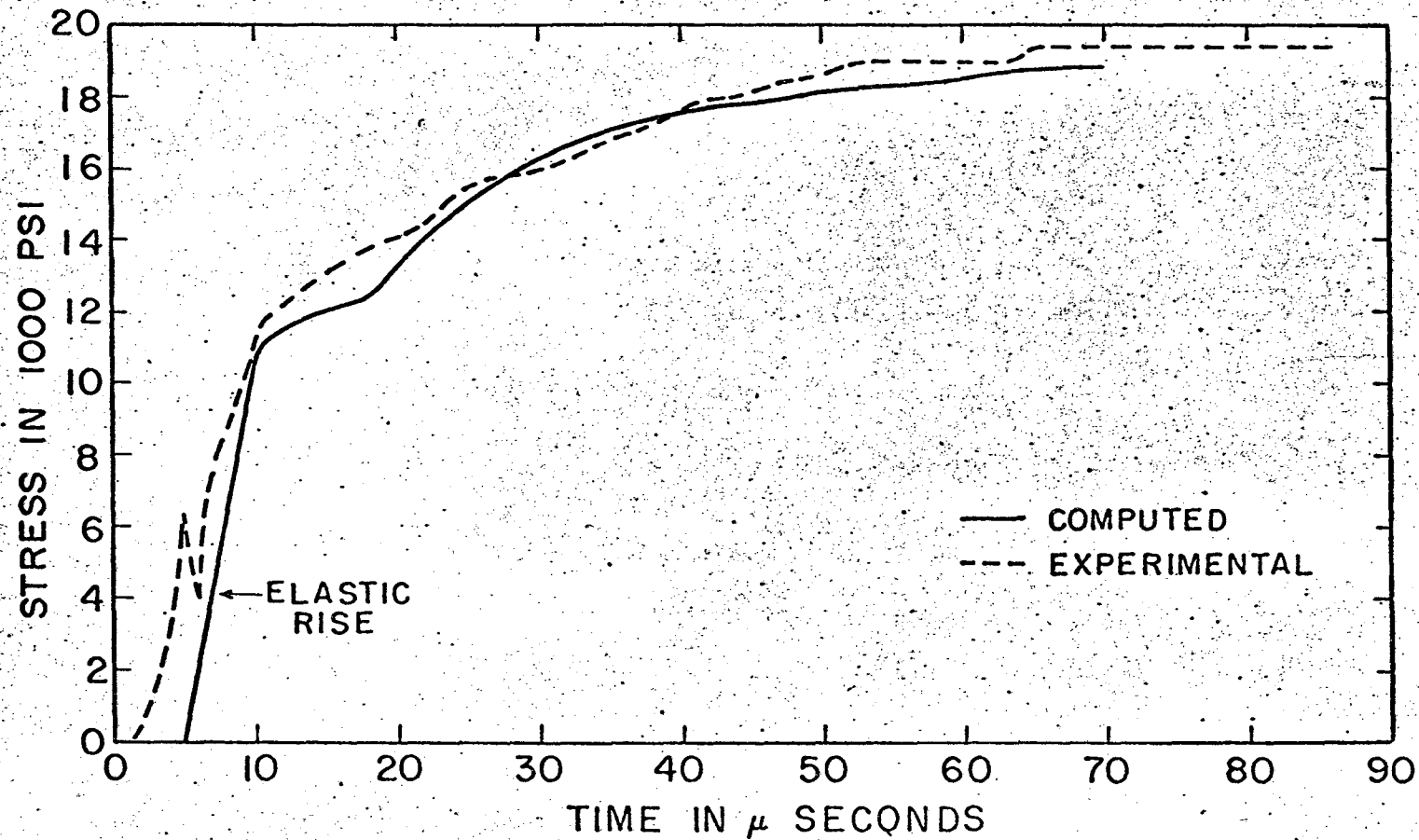


FIG. 6 TRANSMITTED STRESS AT  $\alpha_2$  IN THIN WAFER.

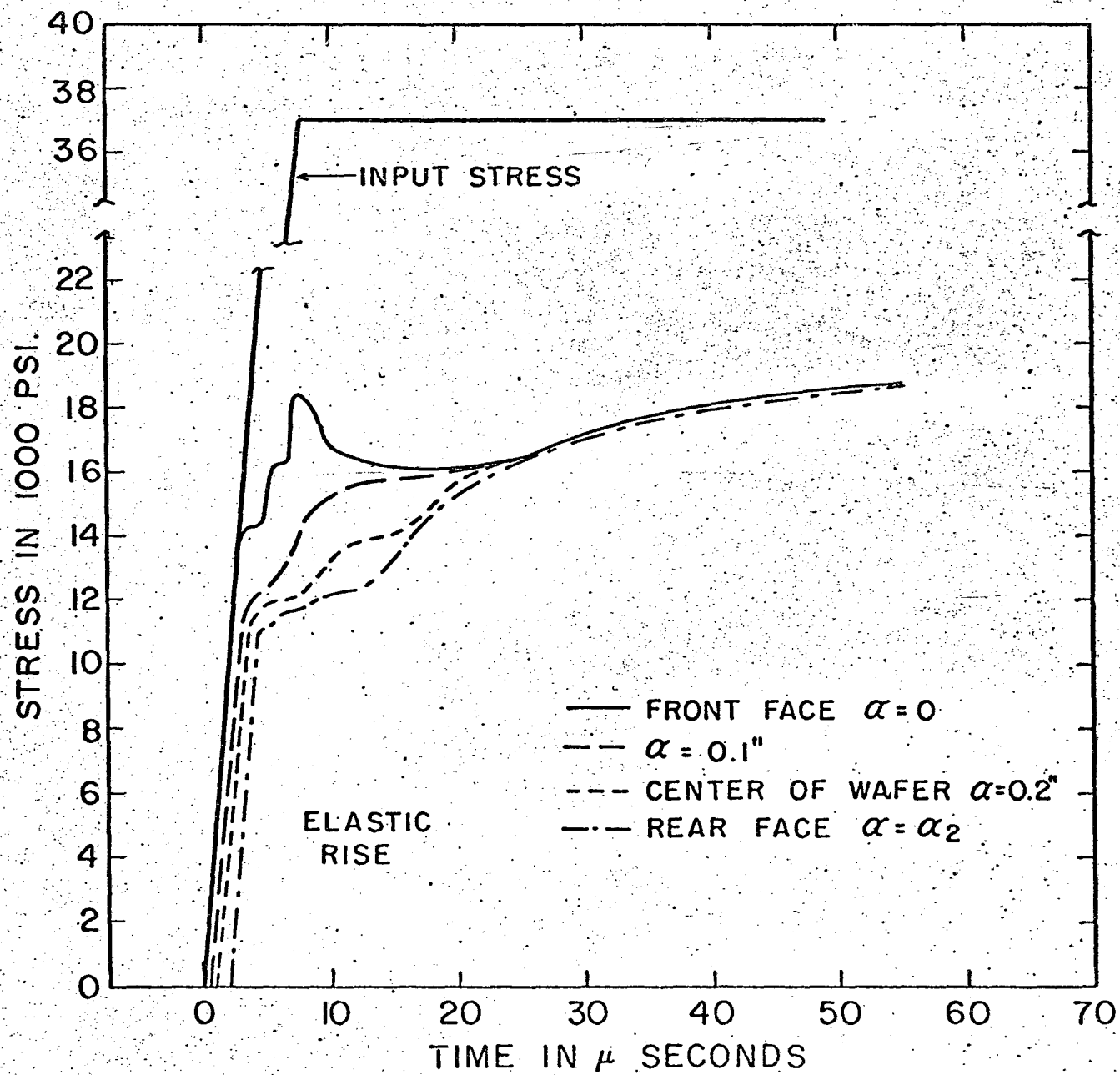


FIG. 7 STRESS IN THIN WAFER.

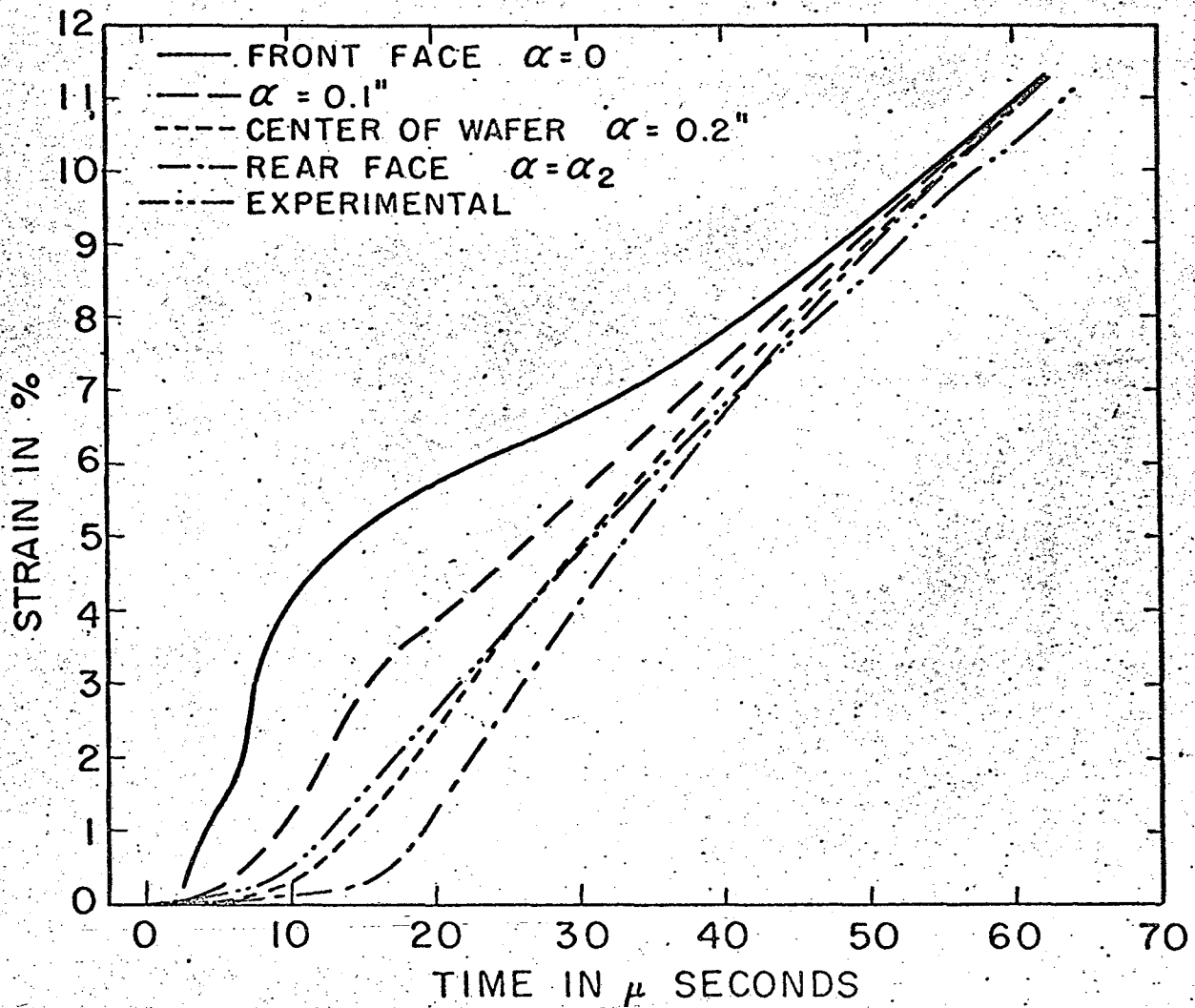


FIG. 8 STRAIN IN THIN WAFER.

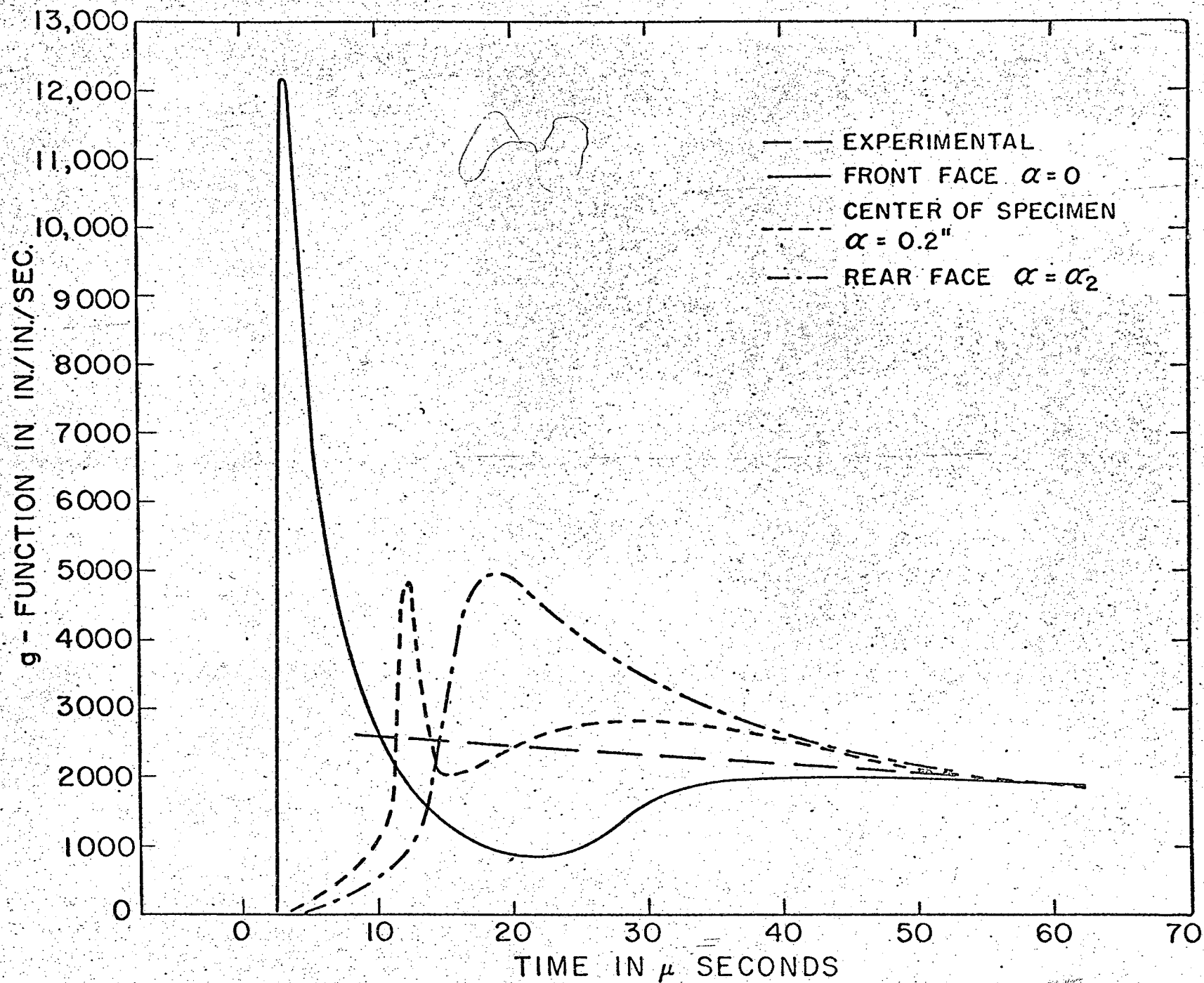


FIG. 9 STRAIN-RATE DISTRIBUTION IN THIN WAFER.

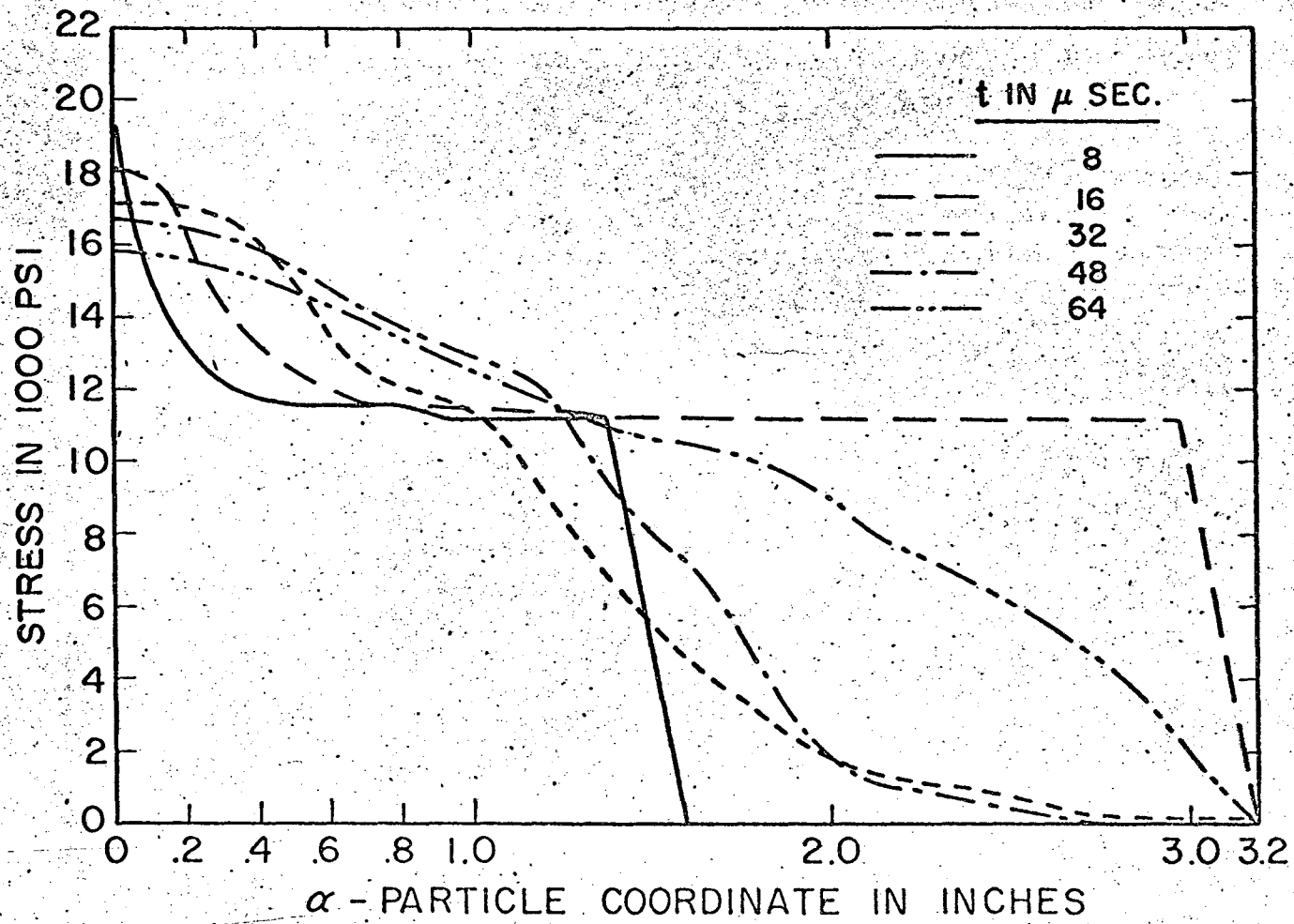


FIG. 10 STRESS DISTRIBUTION IN LONG BAR.

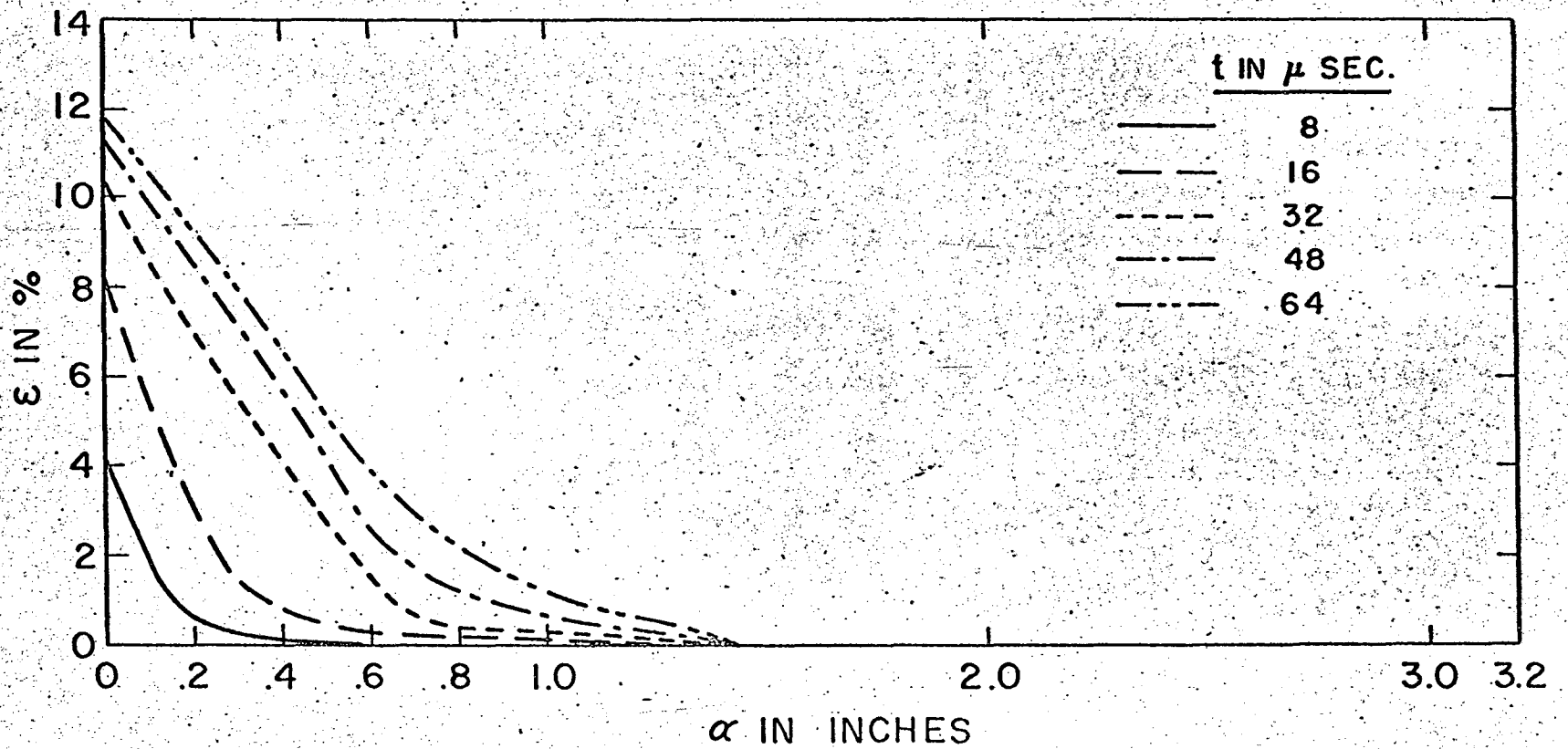


FIG. II STRAIN DISTRIBUTION IN LONG BAR.

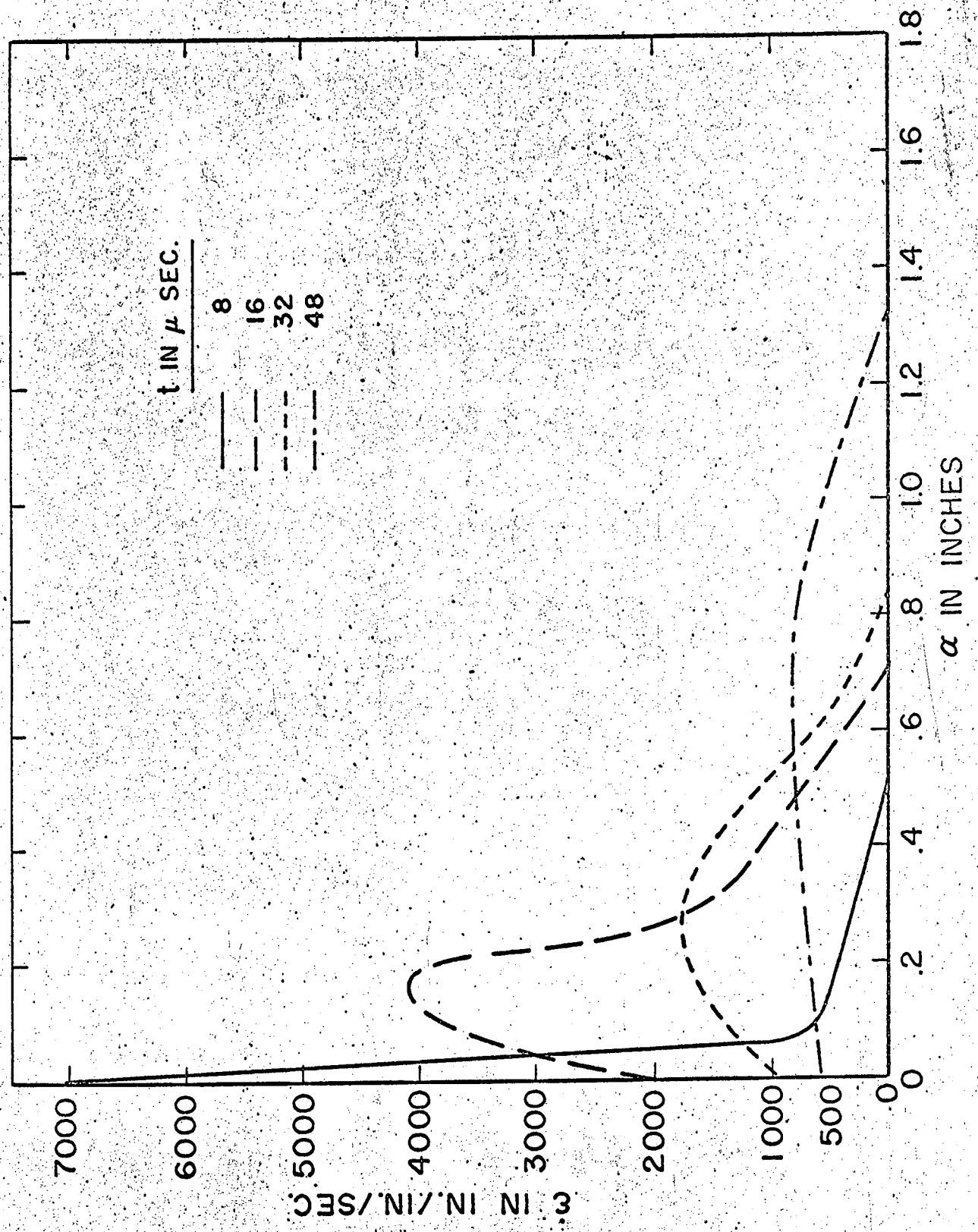


FIG. 12 STRAIN RATE DISTRIBUTION IN LONG BAR.

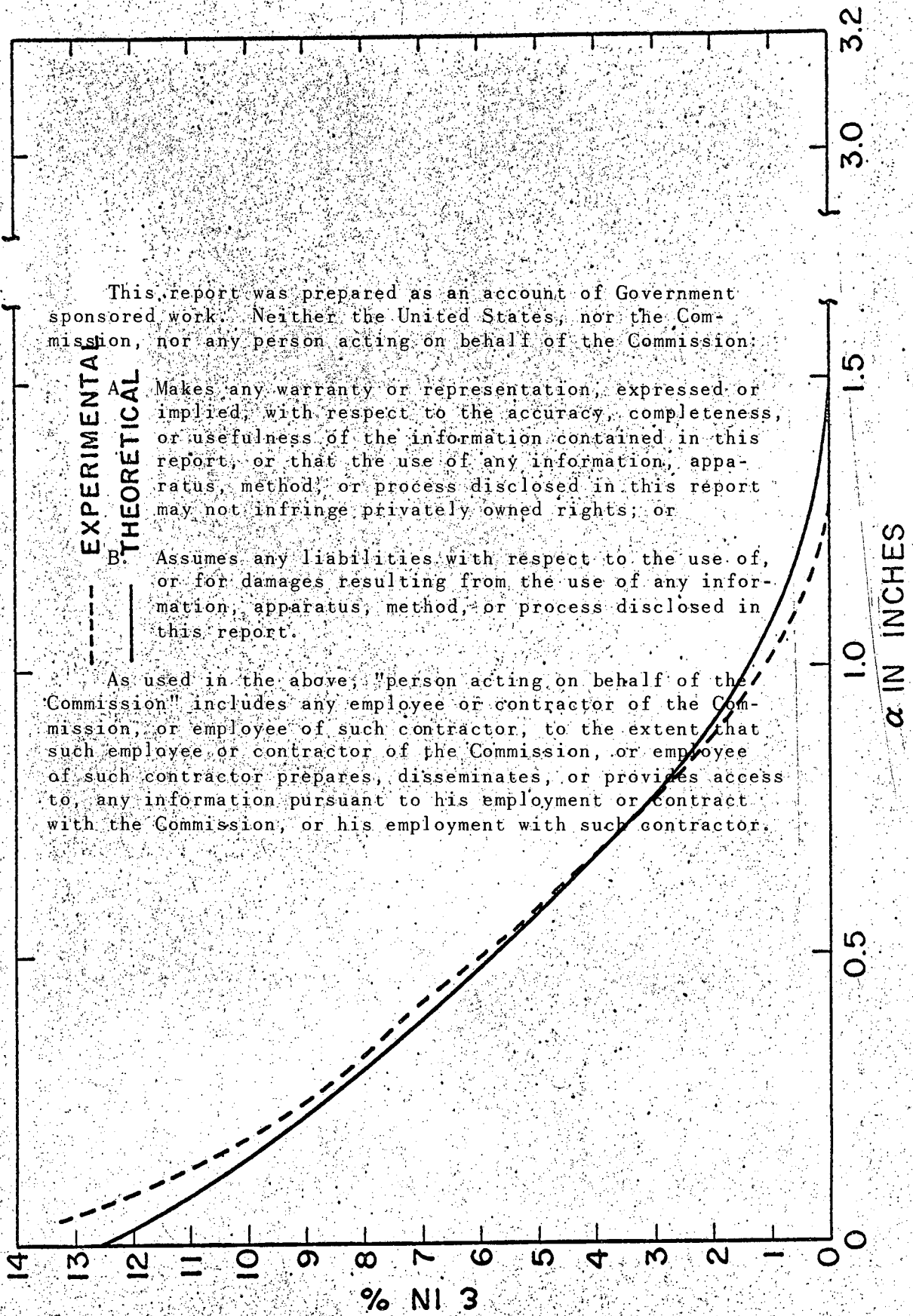


FIG. 13 FINAL STRAIN DISTRIBUTION IN LONG BAR.

This report was prepared as an account of Government sponsored work. Neither the United States, nor the Commission, nor any person acting on behalf of the Commission:

- A. Makes any warranty or representation, expressed or implied, with respect to the accuracy, completeness, or usefulness of the information contained in this report, or that the use of any information, apparatus, method, or process disclosed in this report may not infringe privately owned rights; or
- B. Assumes any liabilities with respect to the use of, or for damages resulting from the use of any information, apparatus, method, or process disclosed in this report.

As used in the above, "person acting on behalf of the Commission" includes any employee or contractor of the Commission, or employee of such contractor, to the extent that such employee or contractor of the Commission, or employee of such contractor prepares, disseminates, or provides access to, any information pursuant to his employment or contract with the Commission, or his employment with such contractor.

